Proanthocyanidin and sodium butyrate synergistically modulate rat colon carcinogenesis by scavenging free radicals and regulating the *COX-2* and *APC* pathways

Elsayed I. Salim[1]* , Sameh M. S. El-Halawany[1], Hanaa A. Hassan[2] and Ezar H. Hafez[1]

Abstract

Background The purpose of this study was to explore the effects of sodium butyrate (NaB), grape seed proanthocyanidin extract (GSPE), or their combination against dimethylhydrazine (DMH)-induced aberrant crypt foci (ACF) formation, which is a proxy for colon carcinogenesis in the rat colon.

Results After inducing colon cancer, all treatments markedly decreased the overall numbers of ACF, with the NaB–GSPE combination eliciting the most pronounced reduction. All the treatments significantly inhibited cell proliferation as indicated by the lower percentages of Ki67-positive cells in the colonic mucosa. Also, caspase-3-immunolabeled cells were found to be significantly increased after all treatments, indicating more apoptotic activity in the initiated colonocytes. Further, the treatments significantly modulated the levels of antioxidant biomarkers, including malondialdehyde, superoxide dismutase, reduced glutathione, and total antioxidant capacity, suggesting a potently induced antioxidant activity, especially after the combination treatment. All treatments, especially the combination, dramatically downregulated the expression of *COX-2* and *APC*, both of which are directly linked to colon cancer.

Conclusions NaB and GSPE exert potent anti-carcinogenic effects, both alone but more effectively in combination, in a rat colon cancer model. They could be important for colon cancer treatment and for adjuvant therapy in humans.

Keywords Colon cancer, Sodium butyrate, Grape seed proanthocyanidin extract, Aberrant crypt foci, *APC*, *COX-2*, Ki67, Caspase-3, Antioxidant activity

Background

Colon cancer or colorectal cancer is the world's third-leading cause of cancer-related mortality and the fourth most-recognized malignancy, accounting for about 935,173 deaths and 1,931,590 new cases in 2020. According to GLOBOCAN 2020, it is the seventh most diagnosed and deadly cancer in Egypt, causing around 5231 new cases and 2852 deaths in 2020 (Sung et al., 2021). While great advances have been made in the treatment and prevention of colon cancer over the last decades, finding new approaches and substances that can be utilized in early cancer intervention is necessary.

Sodium butyrate (NaB), the sodium salt of butyrate, is a short-chain fatty acid that inhibits class I and II histone deacetylases by endogenously binding to their zinc sites, which causes histone hyperacetylation, a change in DNA conformation, and chromatin uncoiling, eventually producing anticancer effects (Abramova et al., 2006). Butyrate also augments the expression of functional genes and proteins involved in the differentiation

*Correspondence:
Elsayed I. Salim
elsayed.salim@science.tanta.edu.eg
[1] Research Lab for Molecular Carcinogenesis, Department of Zoology, Faculty of Science, Tanta University, Tanta 31527, Egypt
[2] Department of Zoology, Faculty of Science, Mansoura University, Mansoura 35516, Egypt

of cells, inducing apoptosis (Li et al., 2015). Butyrate could be why soluble fibers help prevent colon cancer. It affects the development of cancerous as well as normal colon cells in various ways. Butyrate has been shown to suppress the gene expression of the cyclins D1 and E in vitro by inducing G_1/S phase cell cycle arrest, resulting in cellular death. A correlation was reported between butyrate, colon cancer, obesity, and insulin resistance (McNabney & Henagan, 2017). In vivo, NaB combined with Cetuximab® chemotherapy significantly lowered the numbers of rat aberrant crypt foci (ACF) and mucin-depleted foci, proxy markers for colon cancer, and importantly brought the mucus secretion in the colonic mucosa back to normal (Elbassiouni et al., 2018).

Grapeseed extract (GSE) is widely utilized as a dietary supplement to treat various health ailments, including venous insufficiency, wounds, and inflammation. In the United States, the National Center for Complementary and Integrative Health is sponsoring GSE research for Alzheimer's disease and hereditary hemochromatosis. Similarly, the National Cancer Institute in the United States is funding research investigating the use of GSE to prevent lung, colon, and prostate cancers (Gupta et al., 2020). The most active ingredient of GSE, proanthocyanidin, is a strong antioxidant. The in vivo impact of grape seed proanthocyanidin extract (GSPE) on chronic diseases, especially oxidative stress, inflammation, and metabolic syndrome-related disorders, has recently been the focus of much research (Gupta et al., 2020). Better-designed animal experiments with standardized dosages and GSPE composition are needed to more accurately illuminate the cause-effect link between GSPE and its effect on the health of people (Rodríguez-Pérez et al., 2019).

This work aimed to investigate the therapeutic potential of a NaB–proanthocyanidin combination in a rat colon carcinogenesis model, focusing on the underlying histopathological, biochemical, and molecular mechanisms.

Methods
Chemicals and drugs
1,2-dimethylhydrazine dihydrochloride (DMH. 2HCl) and NaB were purchased from Sigma–Aldrich (St. Louis, MO, USA). A highly purified GSPE (HPLC grade, 99.5% pure; proanthocyanidin peak concentration 3634.2 ± 115.7 mg/100 g fresh seed weight) was purchased from The Arab Co. of Pharmaceuticals and Medicinal Plants (MEPACO MEDI FOODS, Enshas El-Raml- El-Sharkeya, Egypt) with the chemical formulation $C_{30}H_{12}O_6$ (CAS Number 84929.27.1).

Rats
Seventy-five healthy, male, 6-week-old Sprague–Dawley rats were bought from Vaccera Co. (Helwan-Giza, Egypt). They were housed in plastic cages with metal grids, wood chips, and eiderdown in the animal facility at Tanta University's Faculty of Science and acclimatized for a week. The experimental design was approved by the Institutional Animal Care Committee at Tanta University's Faculty of Science's Zoology Department (No. IACUC/SCI/TU/0183). The rats were provided free access to tap water and a standard experimental pelleted animal diet. The animals were closely monitored every day, and their body weights, food consumption, and water intake were meticulously recorded every week to identify any indicators of toxicity or abnormalities.

Experimental design
Colon cancer model
For 4 weeks, 60 rats were randomly selected and subcutaneously injected with DMH diluted in a normal 0.9% saline solution at a dose of 40 mg/kg body weight, after their acclimatization period. 15 rats were used as normal control (Salim et al., 2016, 2020).

Experimental groups and treatment
The DMH-injected rats as well as controls were randomly divided into five groups (15 per group) using a RAND () function spreadsheet on Excel (Microsoft office professional plus 2016). Group 1 (G1) was subcutaneously injected with DMH four times and served as a positive control. G2 was administered DMH and then intravenously injected with NaB in 0.9% saline at a dose of 20 mg/kg body weight (Taylor et al., 2019), twice a week until the end of the experiment. G3 was administered DMH and then injected with GSPE thawed in normal saline solution via intragastroluminal gavages at a dose of 300 mg/kg body weight (Cheah et al., 2014), twice a week until the end of the experiment. G4 was administered DMH followed by a combination of NaB and GSPE at the same doses as in G2 and G3, respectively, until the end of the experiment. G5 was injected with the vehicle (0.9% saline) and served as the normal control group.

All treatments started 2 days after the last carcinogen injection. NaB was administered intravenously because it is absorbed rapidly into the upper gastrointestinal tract if taken "free" (no-compound form). It must reach the colon for the most beneficial effect (Bedford et al., 2017).

After 16 weeks, all the rats were sacrificed following anesthesia with excess ethyl ether. During the sacrifice,

Salim *et al. The Journal of Basic and Applied Zoology*   (2023) 84:24

Page 3 of 10

they were examined grossly and macroscopically. After the organs were necropsied, the absolute and relative organ weights (%) were calculated per the following formula: organ weight/body weight × 100.

Preparation of the colon for ACF counting

The entire colon was removed during necropsy, inflated with cold saline, opened longitudinally, and rinsed in saline. Briefly, the cecum was removed and the colon was separated into three segments, each representing one of three colonic regions: proximal, middle, and distal colon. Each segment's length and width were calculated followed by fixing them flat on a filter paper for at least 48 h at 4 ℃ in fresh 10% phosphate-buffered formalin, washing them, and staining them with 0.1% methylene blue in water for 3 min to count ACF (Salim et al., 2019). Two pathologists examined the specimens under a light microscope at 200× and 400× magnifications with the mucosal side facing up. ACF with different multiplicities were counted and divided into groups based on the number of crypts: foci containing 1 crypt (1 AC), 2 AC, 3 AC, or 4 AC. The quantity of ACF, their distribution patterns, and the colon and crypt multiplicities were determined. Colons from each rat were fixed in paraffin, stained with hematoxylin and eosin, and evaluated for histopathological and immunohistochemical (IHC) alterations after ACF counting.

IHC investigation of Ki67 and caspase-3 levels

In 4-μm sections of each area of the colon tissues, the avidin–biotin complex technique was used to evaluate Ki67 and caspase-3 levels (Hsu, 1981). Briefly, IHC was performed on at least 10 sections from 10 different rats, two out of the three parts of each colon. To calculate the labeling indices (LI%) for the specific antibodies, the total number of positively stained nuclei or cells in all complete crypts detected in each section was tallied and divided by the total number of nuclei in each crypt (%). The IHC results were analyzed by two animal pathologists who were unaware of the experimental groups.

Measurement of antioxidant enzyme activities

The lipid peroxidation level of malondialdehyde (MDA) was measured according to Yoshioka et al (1979). The superoxide dismutase (SOD) activity in serum was measured using the method of Shiraishi et al (2005), and reduced glutathione (GSH) concentration was evaluated using the method of Vobornikova and Pohanka (2016). The total antioxidant capacity (TAC) was determined using a kit according to the manufacturer's protocol (Abnova kit, Walnut, CA. 91788, USA).

Quantitative reverse transcription-polymerase chain reaction (qRT-PCR) analysis for *APC* and *COX-2*

The mRNA levels of *APC* and *COX-2* were estimated using qRT-PCR. The housekeeping gene *β-Actin* was used as a reference. The sequences of primers used are listed in Table 1. The colon was cut longitudinally, and the layer of mucosa was scraped using clean slide glasses from the inner lining of the colon and stored at −80 °C until the required analyses were performed. A complete RNA isolation kit (Analytika Jena, Germany) was used to extract RNA from the mucosa according to the manufacturer's instructions. Sensiscript Reverse Transcriptase (Synthesis Kit) was used to make single-stranded complementary DNA from 100 ng of pure RNA using random hexamers, according to the manufacturer's instructions.

The Applied Biosystems Step One™ Instrument was used for all PCR experiments. To avoid inter-run variance, samples from the same group were always run together. Preliminary tests were carried out before the main experiment to establish the best primer concentrations, SYBR Green RT-PCR reactants, and reaction conditions. Hot Start was used to perform qRT-PCR reactions. QIAGEN Taq DNA Polymerase was modified to create Taq DNA Polymerase.

Analysis of qRT-PCR data

The threshold cycle (C_T) was utilized to determine the level of gene expression in all the different treatment groups. Applied Biosystems Step One™ Instrument software was then used to calculate the gene expression level.

Table 1 The primer's nucleotide sequences of the rat colon cancer-related genes and housekeeping gene

Gene	Rat primer sequence (5′–3′)	Size of PCR product	Gene accession number
β-actin	F: 5′-AGGATGCGTCCACCAAGAAG-3′ R: 5′-TGTCCAGCCCATGATGGTTC-3′	249 bp	NM_001101.3
COX-2	F: 5′- TGGTGCCGGGTCTGATGATG-3′ R: 5′- GCAATGCGGTTCTGATACTG -3′	252 bp	NC_005112.4
APC	F: 5′- CAGACTCCAAAAGGGACTGC-3′ R: 5′- TGAATACAAGGGGCGTCTCC -3′	297 bp	NC_005117.4

All primer sequences were obtained from the gene bank of NCBI BLAST

The results were expressed as the ratio of reference gene to target gene expression using the following formula: ΔC_T (number of cycles at the threshold level of a log-based fluorescence/normalized to endogenous control genes) = C_T (target genes) – C_T (control genes). The relative expression levels were determined according to the following formula: $\Delta\Delta C_T = \Delta C_T$ (Treated) — ΔC_T (Control). Consequently, the expression values were expressed as n-fold variations in relation to the calibrator. The expression of the concerned genes was calculated as $2^{-\Delta\Delta CT}$ using Microsoft Excel software.

Blinding was used for each step of the experimental process such as allocation, the conduct of the experiment, the assessment of the outcomes, and during the data analysis.

Statistical analyses

Group values expressed as means ± standard deviations were evaluated by the *t*-test or analysis of variance while percentage data were analyzed by the chi-squared test using Statistical Package for Social Science ver. 17 (USA). $P < 0.05$ was considered to be statistically significant.

Results

Average body weight and absolute and relative organ weights

No mortality was recorded until the end of the experiment. All animals remained healthy and were included in the experiment without any exclusion. The final body weights were comparable among all groups except G4

(NaB + GSPE following DMH), wherein the animals showed significantly decreased body weights compared with those in G2 (DMH only). Moreover, the average relative spleen weights in the DMH-only group were considerably higher than in the normal control group, but all treatments lowered the absolute spleen weights to near-normal levels. The relative organ weights did not differ considerably between the groups (Fig. 1, Table 2).

Effect of NaB, GSPE, or their combination on average numbers of ACF

Morphologically, the ACF varied in size and shape: some were only one big aberrant crypt (1 AC), while others were clustered in foci containing 2 ACs, 3 ACs, or larger aberrant crypts (≥ 4 ACs) in one focus. The incidence of ACF was 100% in all DMH-treated animals. Calculations for the ACF criteria are shown in Table 3. In comparison to the other DMH-treated groups, G1 had the greatest total ACF counts, while the numbers of ACF observed in G2 and G3 were significantly lower than those found in G1. Treating DMH-induced rats with NaB, GSPE, or their combination significantly reduced the total number of aberrant crypts as well as the number of 1, 2, 3, and 4 ACs when compared with the DMH-treated group (Fig. 2).

Histopathological findings in the colonic epithelium

Histological examination of hematoxylin and eosin-stained colonic epithelia from different groups revealed that G1 rats showed slight to moderate dysplasia,
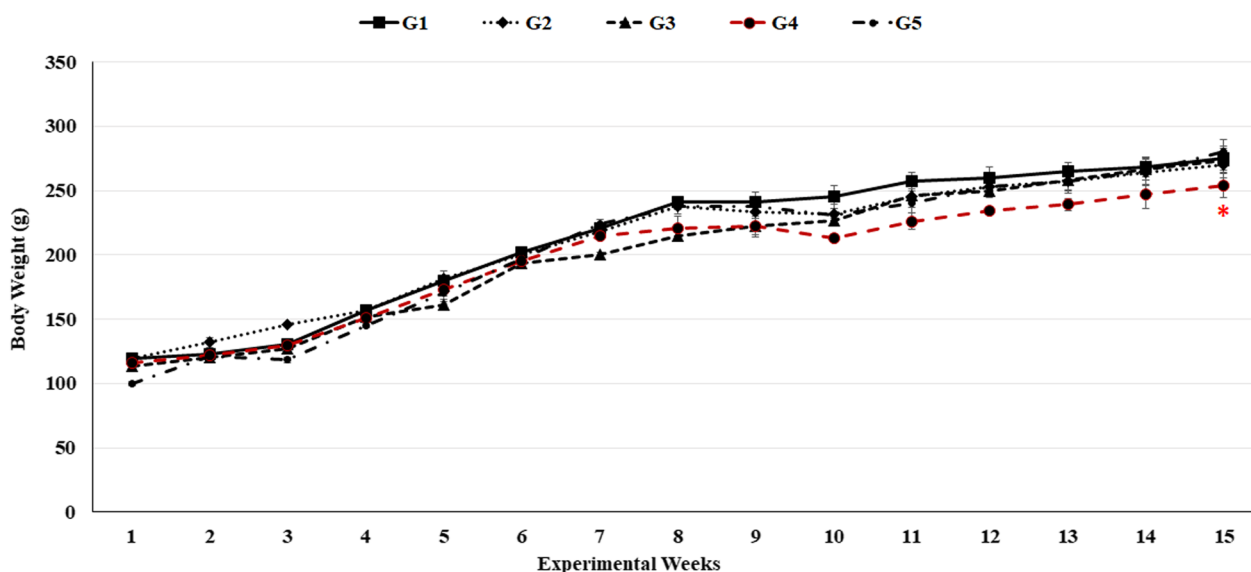

Fig. 1 Average body weight curves for rats in all experimental groups. G1: DMH, G2: DMH + NaB, G3: DMH + GSPE, G4: DMH + NaB + GSPE, and G5: normal control. *****G4 is significant versus G1 at P < 0.05 (ANOVA). Data of 15 rats/ group are shown. DMH, 1,2-dimethylhydrazine; NaB, sodium butyrate; GSPE, grape seed proanthocyanidin extract; ANOVA, analysis of variance

Salim *et al. The Journal of Basic and Applied Zoology*   (2023) 84:24

Page 5 of 10

Table 2 Final body, absolute and relative organ weights

Group/treatment	Final body wt (g)	Liver wt (g)	R. Kidney wt (g)	L. Kidney wt (g)	Spleen wt (g)
G1 (DMH)	275 ± 27 [a]	6.49 ± 0.84 (2.36)[b]	0.72 ± 0.11 (0.26)	0.74 ± 0.09 (0.27)	1.03 ± 0.18* (0.37)
G2 (DMH + NaB)	270 ± 22.3	6.19 ± 0.93 (2.29)	0.72 ± 0.11 (0.26)	0.74 ± 0.11 (0.27)	0.86 ± 0.12 * (0.31)
G3 (DMH + GSPE)	273 ± 28.3	6.24 ± 0.93 (2.28)	0.74 ± 0.11 (0.27)	0.76 ± 0.16 (0.27)	0.88 ± 0.15* (0.32)
G4 (DMH + NaB + GSPE)	254 ± 26.9*	6.18 ± 0.98 (2.43)	0.73 ± 0.16 (0.28)	0.74 ± 0.20 (0.29)	0.87 ± 0.2* (0.34)
G5 (normal control)	277 ± 13.4	5.71 ± 0.9* (2.06)	0.70 ± 0.08 (0.25)	0.69 ± 0.0* (0.25)	0.79 ± 0.15* (0.28)

[a] Mean ± S.D

[b] No. in parentheses is relative organ wt.: ratio of organ wt/body wt (%)

*Significant versus G1 at P < 0.05 (ANOVA, analysis of variance); DMH: 1, 2-dimethylhydrazine; NaB: Sodium butyrate; GSPE: Grapeseed proanthocyanidin extract. Data of 15 rats/ group are shown.;

Table 3 Mean numbers of aberrant crypt foci (ACF)

Group/treatment	Total no. of ACF	No. of foci containing:			
		1 AC	2 ACs	3 ACs	≥ 4 ACs
G1 (DMH)	208 ± 34.8[a]	92.4 ± 12.1	59.3 ± 14.1	35.7 ± 0.1	20.1 ± 7.1
G2 (DMH + NaB)	91.6 ± 24.2*	41.4 ± 10.3*	24.4 ± 8.4*	16.0 ± 3.8*	9.7 ± 3.2*
G3 (DMH + GSPE)	96.3 ± 21.5*	43.0 ± 10.9*	13.8 ± 6.9*	8.75 ± 2.1*	7.50 ± 1.3*
G4 (DMH + NaB + GSPE)	52.3 ± 13.2*	26.1 ± 6.1*	15.6 ± 3.7*	7.6 ± 2. 7*	2.8 ± 13.2*

[a] Means ± standard deviations

*Significant versus G1 at P < 0.05 (ANOVA); ACF: Aberrant crypt foci; DMH: 1,2-dimethylhydrazine; NaB: Sodium butyrate; GSPE: Grapeseed proanthocyanidin extract. Samples from 10 rats/group were subjected to the ACF analysis assay
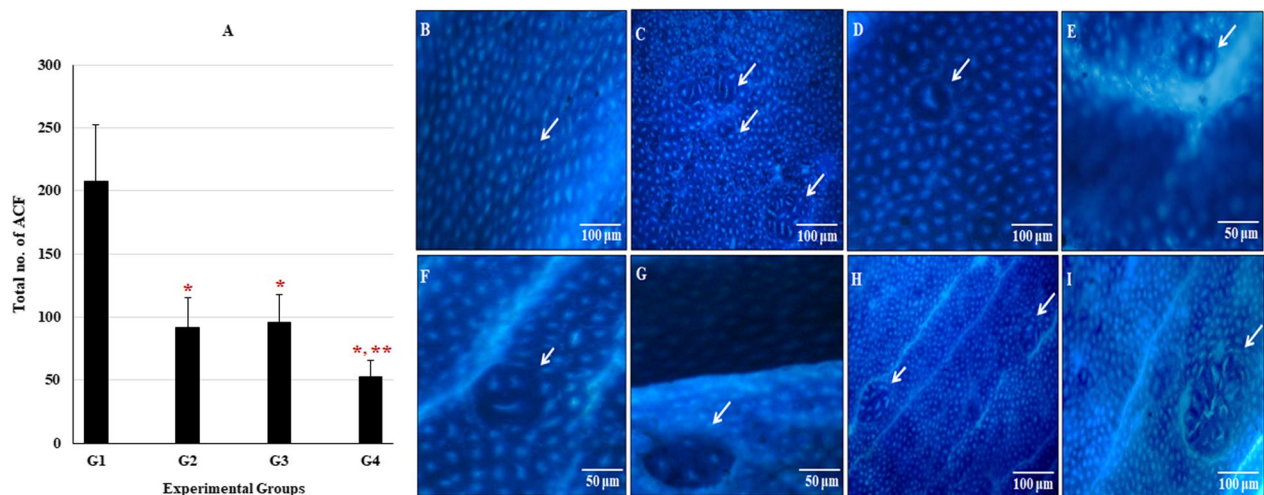

Fig. 2 **A** Average total numbers of ACF observed in the colons of rats from all experimental groups; *****significance versus G1 at P < 0.05; ******significance vs. G2 and G3 at P < 0.05 (ANOVA); samples from 10 rats/group were subjected to the ACF analysis assay. **B–I** Photomicrographs of whole colons stained with methylene blue. **B** normal epithelium with normal crypts; **C** colonic epithelium of a rat injected with DMH showing aberrant crypts; **D** a focus with 1 aberrant crypt (1 AC); **E** a focus with 2 ACs; **F** a focus with 3 ACs; **G** a focus with 4 ACs; **H** a focus with ≥ 4ACs; **I** a magnified portion of **H**. ACF, aberrant crypt foci

Salim *et al. The Journal of Basic and Applied Zoology*   (2023) 84:24

Page 6 of 10

increased numbers of lymphocytes in intra-cryptal zones, slightly elongated crypts, and comparatively lesser mucin-secreting cells. None of these histopathological changes were observed in the colonic epithelia of normal rats. Treatment with NaB, GSPE, or their combination induced a marked decrease in dysplasia, lowered the extent of lymphocytic infiltration, produced shorter to normal length colonic crypts, and increased the number of mucin-secreting cells. These recovery changes were most obvious in G4, the combination treatment group (Fig. 3C–G).

Changes in Ki67 in the colonic epithelium
In comparison to the other groups, Ki67 LI (%) was the highest in G1 (Fig. 3A). In addition, DMH injection lengthened the proliferative zone in the colonic crypts, as evidenced by increased numbers of tagged cells in the upper third of the crypts as compared with the normal control (Fig. 3H–L). The four DMH-injected groups showed statistically significant differences when compared with the normal control. Treatment with NaB, GSPE, or their combination significantly reduced the Ki67 LI (%) when compared with that in G1. Moreover, compared with G2 and G3, the Ki67 LI (%) in G4 was dramatically reduced (Fig. 3A).

Changes in caspase-3 in the colonic epithelium
The staining was predominantly nuclear and limited to the epithelial cells of the colonic crypt walls; however, it was also visible in some intra-cryptal cells in the
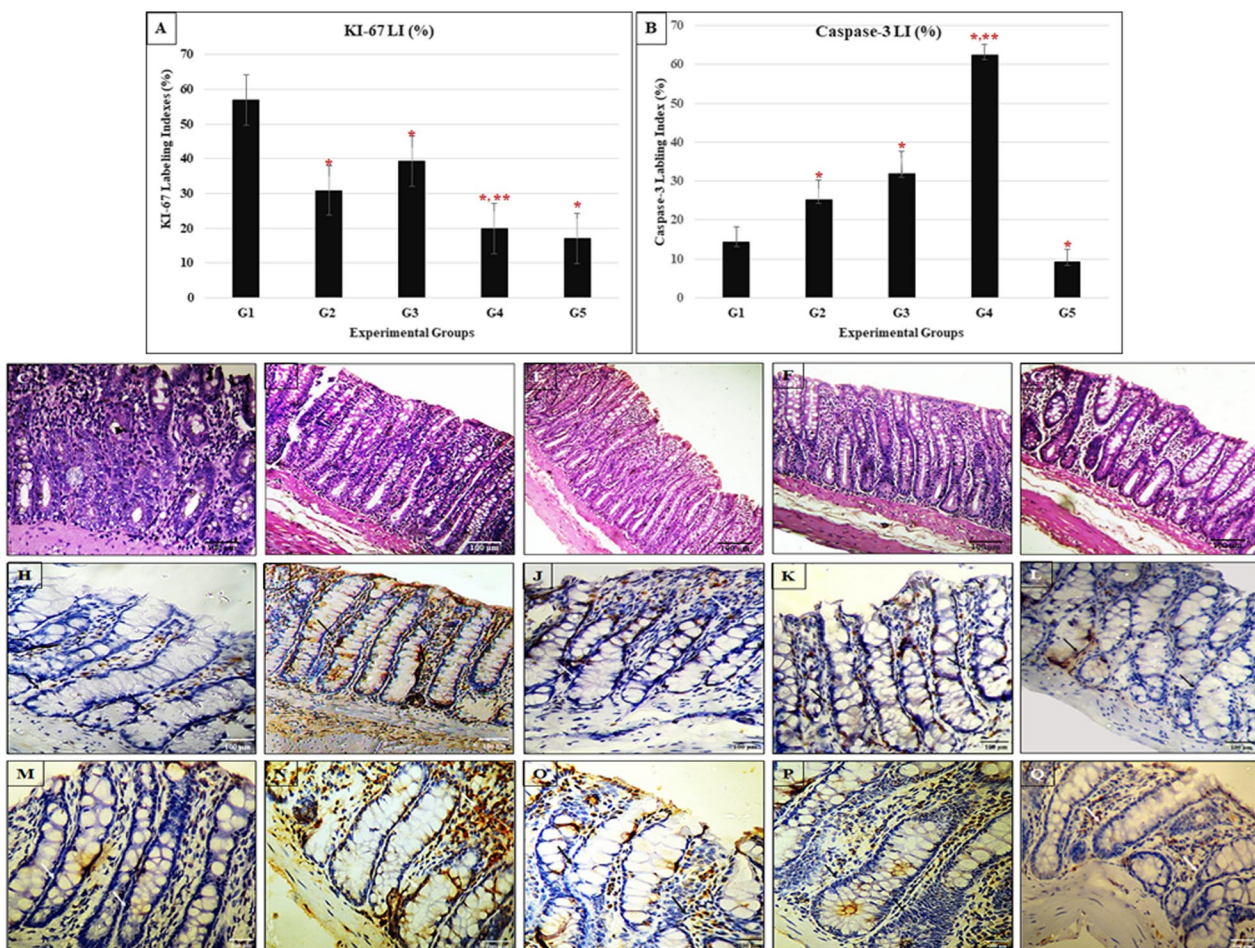

Fig. 3 **A**, **B** Calculated IHC labeling indexes (%) of Ki67 (**A**) and caspase-3 (**B**); *significance vs. G1 at P < 0.05; **significance versus G2 and G3 at P < 0.05 (ANOVA); samples from 10 rats/group were subjected to IHC analysis. **C**–**G** Photomicrographs of hematoxylin and eosin-stained rat colonic epithelia; **C** DMH-administered control (G1); **D** DMH + NaB-treated rats (G2); **E** DMH + GSPE-treated rats (G3); **F** DMH + NaB + GSPE-treated rats (G4); **G** normal control (G5). 10 rats/group were subjected to hematoxylin and eosin staining. **H**–**L** IHC staining photomicrographs of Ki67. **H** DMH-injected rats; **I** DMH + NaB-treated rats; **J** DMH + GSPE-treated rats; **K** DMH + NaB + GSPE-treated rats; **L** normal control. **M**–**Q** IHC staining photomicrographs of caspase-3. **M** DMH-injected rats; **N** DMH + NaB-treated rats; **O** DMH + GSPE-treated rats; **P** DMH + NaB + GSPE-treated rats; **Q** normal control. IHC, immunohistochemistry

Salim *et al. The Journal of Basic and Applied Zoology*   (2023) 84:24

Page 7 of 10

submucosal areas (Fig. 3M–Q). Caspase-3 LI (%) was moderately detected in G1 rats (14.2%). Treatment with NaB or GSPE significantly increased caspase-3 LI (%) to 25.2% and 31.9%, respectively (Fig. 3B). The combination treatment induced the highest increase of 62.3% among the treatment groups (P < 0.05).

Serum levels of oxidative stress markers

Compared with the normal control group, MDA activity was significantly lower in all the treatment groups. The combination treatment significantly inhibited MDA activity compared with DMH treatment, while individual treatment with NaB or GSPE brought it to a level similar to that after DMH treatment. On the other hand, SOD activity in all the treatment groups was significantly higher than in the normal control, with G4 showing a significantly higher SOD activity than all the other groups. Further, G2–4 showed significantly higher GSH levels compared with G1, with G4 showing the least increase among them. The TAC levels were at their minimum in normal control rats while G2 and G3 rats exhibited a significant increase in TAC compared with G1 rats (Fig. 4).

COX-2 and APC gene expression

G1 rats showed a significant increase in *COX-2* expression compared with G2–4 rats. *COX-2* was significantly downregulated by ninefold in G2 rats and by almost fourfold in G3 rats. The combination treatment affected a 22-fold decrease in *COX-2* expression. Similarly, *APC* expression was considerably higher in G1 rats than in the other groups. It was downregulated by 2.5-fold in G2, sevenfold in G3, and 14-fold in G4 (Fig. 5).

Discussion

Accumulative data have shown previously that ACF can be used successfully in human chemoprevention studies (Roncucci et al., 2000). ACF was successfully induced in this study. The numbers of large and small foci were significantly reduced after treatment with NaB or GSPE, while the greatest decrease was recorded after the combination treatment.

NaB exerts several biological effects within the cellular matrix: it inhibits replication, induces differentiation, and modulates gene expression. Being a short-chain fatty acid that includes cellulose acetate, it regulates cell cycle kinetics (Ma et al., 2018). ACF formation was found to decrease more significantly when the diet of rats was supplemented with fish oil/butyrate compared with maize oil/butyrate (Kruh, 1981). This study suggests that butyrate's protective mechanism against colon carcinogenesis could rely on nutritional fat and other mechanisms that need exploration.

The current study shows that the inhibitory effects of NaB, GSPE, or their combination on colon carcinogenesis
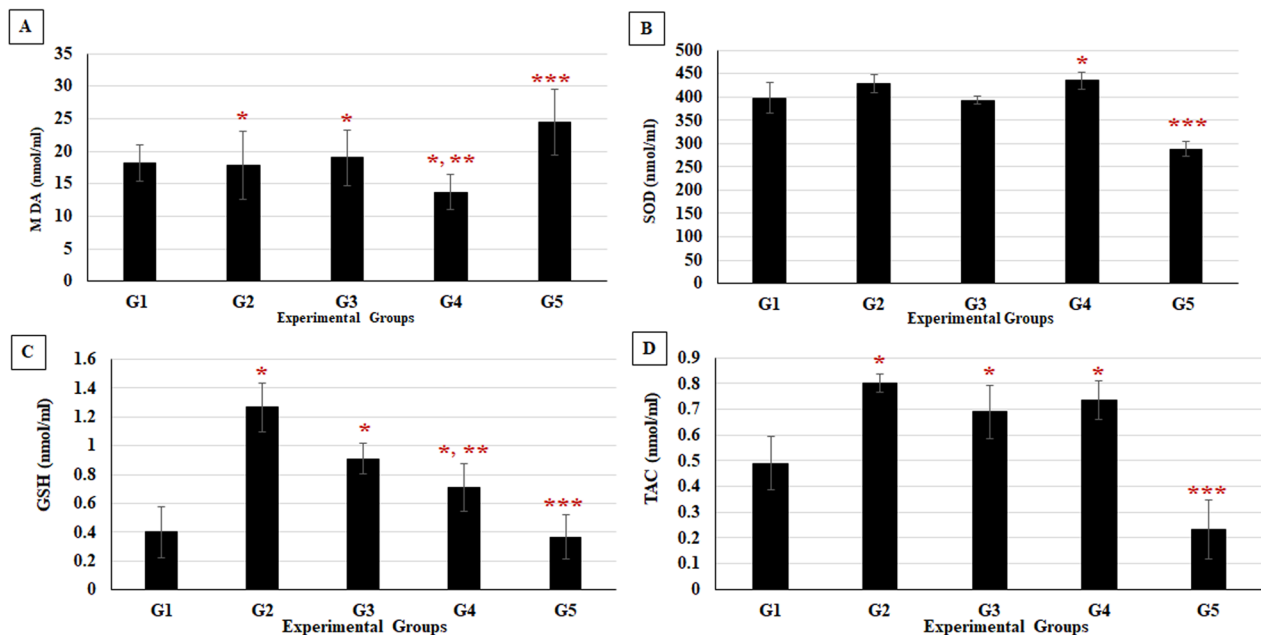

Fig. 4 Antioxidant enzyme activities in the sera of normal and treated rats. **A** lipid peroxidation activity (MDA); **B** SOD activity; **C** GSH activity; **D** TAC levels. ***Significance versus G1 at P < 0.05; ****significance versus G2 and G3 at P < 0.05; *****significance versus G1, G2, G3, and G4 at P < 0.05 (ANOVA). Samples from 5 rats/group were subjected to the antioxidant enzyme activity assay. MDA, malondialdehyde; SOD, superoxide dismutase; GSH, reduced glutathione; TAC, total antioxidant capacity
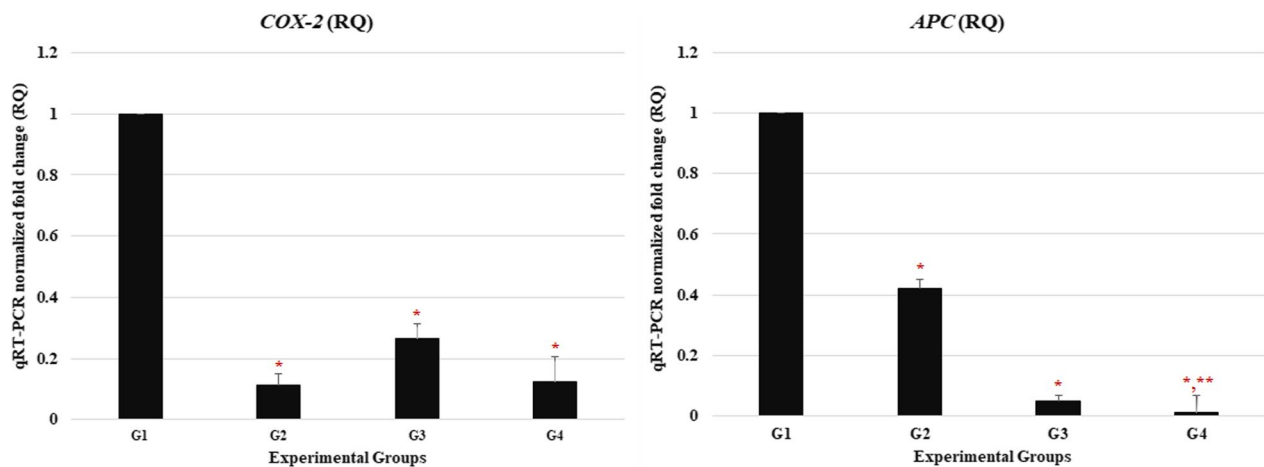
Fig. 5 qRT-PCR normalized fold change data for mRNA expression in the studied groups. **A** *COX-2* gene expression; **B** *APC* gene expression in the studied groups; *****significance versus calibrator (G1) at P < 0.05 (*t*-test). ******significance vs. G2 and G3 at P < 0.05 (ANOVA); Samples from 5 rats/group were subjected to the qRT-PCR assay. qRT-PCR, quantitative reverse transcription-polymerase chain reaction; COX-2, cyclooxygenase-2; APC, adenomatous polyposis coli

are associated with a subsequent inhibition of cell proliferation in the colonic epithelium, which may have contributed significantly toward reducing the number of ACF and may eventually prevent polyp formation and colonic tumors. GSPE has been demonstrated to inhibit the proliferation of several cancer cells, including colon cancer cells, as well as to elicit an increased drug response (Cheah et al., 2014). Dimers, trimers, and other oligomers of flavan-3-ols found in GSPEs are known to possess antiproliferative properties (Cheah et al., 2014). Also, NaB alone has been shown to attenuate cell proliferation in rat colons during carcinogenesis (Medina et al., 1998). In a recent study, the number of Ki67-positive cells was considerably lower in rats treated with black grape extract than in the untreated group (Yang et al., 2020).

Our caspase-3 IHC results are consistent with those of Ghareeb et al. (2018), who demonstrated that DMH injection decreased the expression of the apoptotic markers P53 and caspase-3, subsequently supporting higher cell proliferation levels in the colon epithelium. In a recent study, qPCR results showed that caspase-3 expression in the GSPE-treated population was much higher than in the control groups (Guo et al., 2018). By stimulating caspase, degenerating mitochondrial membrane potential, and triggering cytochrome C release, GSPE could induce apoptosis in the human prostate cancer cells, DU145 (Agarwal et al., 2002). Contrarily, Tu et al. (2019) postulated that GSPE can inhibit apoptosis by preventing the activation of Bax and caspase-3. GSPE exerts antioxidant, anti-inflammatory, and anticancer effects. NaB was found to promote apoptosis by lowering Bcl-2, elevating Bax, decreasing survivin, and activating

caspase-3 (Taylor et al., 2019). These findings justify the apoptosis-inducing effects exerted by both treatments in the rat colonic epithelia.

Oxidative stress is linked to the incidence and progression of various cancers (Wu et al., 2017). In this study, NaB, GSPE, or their combination significantly affected the serum activities of MDA, SOD, GSH, and TAC. Consistent with the present results, a previous study showed that GSPE modulated the serum levels of SOD, glutathione peroxidase, TAC, catalase, and MDA in a linear fashion (Ao & Kim, 2020). GSPE oil effectively regulates the antioxidant protection mechanism by inhibiting lipid peroxidation and enhancing antioxidant enzyme activities (Belviranl et al., 2012). We have previously published similar results documenting the antioxidative stress potential of GSPE in rat liver carcinogenesis (Sherif et al., 2017).

The present data agree with previous studies which reported elevated MDA levels in rat serum after administration of azoxymethane (Sharma et al., 2018) or DMH (Manju et al., 2005). The ability of the GSPE–NaB combination to inhibit MDA formation is indicative of its anti-carcinogenic effect. The significant elevation in SOD activity further supports this conclusion. SOD serves to defend against the potentially harmful reactivates of superoxide and hydrogen peroxide. Also, both GSPE and NaB increased the GSH activity. In a previous study, DMH was found to decrease GSH antioxidant potential in rats (Saleem et al., 2019). Our findings about TAC levels being increased after all treatments corroborate those of El-Kholy et al. (2017), who showed that many therapies induced an increase in TAC in the heart and liver.

Salim *et al. The Journal of Basic and Applied Zoology*   (2023) 84:24

Page 9 of 10

COX-2 is mainly expressed in cancerous conditions via the activation of inflammatory cytokines (Umesalma & Sudhandiran, 2010). By inhibiting apoptosis and enhancing cancer-induced angiogenesis, it promotes cancer cell proliferation (Wendum et al., 2004). The present *COX-2* gene expression results are consistent with those of Mao et al. (2016), who reported that GSPE exerts antineoplastic properties by inhibiting the *COX-2*–prostaglandin E2 eicosanoid pathways. NaB has also been shown to downregulate *COX-2* expression (Jia et al., 2020). In our study, the combination of NaB and GSPE was the most efficient in reducing the expression of *COX-2*. Similarly, while the expression of *APC* was downregulated by all treatment groups in this study, the combination treatment was the most efficient. The colonic *APC* gene has been shown to get mutated after DMH administration in rats during the early stages of initiation (Sohn et al., 1999). Our data is consistent with previous studies involving the use of nutraceuticals against DMH-induced colon carcinogenesis (Sadik & Shaker, 2013).

Conclusions

NaB and GSPE exert direct therapeutic effects on most biomarkers of rat colon carcinogenesis and they are strongly related to the metabolic processes within cells. The results at the genetic level are associated with the phenotypes of the various stages of colon carcinogenesis. Therefore, NaB and GSPE could play important therapeutic roles in the targeted treatment of precancerous colon cells.

Abbreviations

ACF	Aberrant crypt foci
APC	Adenomatous polyposis coli
C_T	Threshold cycle
COX-2	Cyclooxygenase-2
DMH	1,2-Dimethylhydrazine
GSH	Reduced glutathione
GSE	Grapeseed extract
GSPE	Grapeseed proanthocyanidin extract
IHC	Immunohistochemistry
LI	Labeling indices
MDA	Malondialdehyde
NaB	Sodium butyrate
SOD	Superoxide dismutase
TAC	Total antioxidant capacity
qRT-PCR	Quantitative reverse transcription-polymerase chain reaction

Author contributions
ES set the conception and the experimental design, was a major contributor to writing the manuscript and performed the pathological, molecular analysis, and data interpretation; SE performed the animal caring and data analysis and contributed to writing the manuscript. HH has planned and revised the physiological analysis, and EH did the statistics and assisted in the preparation and revision of the text. All authors have agreed to be personally accountable for their contributions. And to ensure that any questions about the accuracy or integrity of any part of the work, even if they were not personally involved, are appropriately investigated, resolved, and the resolution documented in the literature.
The final manuscript was read and approved by all writers.

Availability of data and materials
All data generated or analyzed during this study are included in this published article.

Declarations

Ethics approval and consent to participate
The Institutional Animal Care Committee at Tanta University's Faculty of Science's Zoology Department approved the design of this study (No. IACUC/SCI/TU/0183).

Consent for publication
Not applicable.

Competing interests
There are no competing interests declared by the authors.

References

Abramova, V. M., Pospelova, V. T., Nikulenkov, P. F., et al. (2006). G1/S arrest induced by histone deacetylase inhibitor sodium butyrate in E1A + Ras-transformed cells is mediated through down-regulation of E2F activity and stabilization of beta-catenin. *Journal of Biological Chemistry, 281*(30), 21040–21051.

Agarwal, C., Singh, R. P., & Agarwal, R. (2002). Grape seed extract induces apoptotic death of human prostate carcinoma DU145 cells via caspases activation accompanied by dissipation of mitochondrial membrane potential and cytochrome c release. *Carcinogenesis, 23*(11), 1869–1876.

Ao, X., & Kim, I. H. (2020). Effects of GSE on performance, immunity, antioxidant capacity, and meat quality in Pekin ducks. *Poultry Science, 99*(4), 2078–2086.

Bedford, A., Yu, H., Squires, E. J., Leeson, S., & Gong, J. (2017). Effects of supplementation level and feeding schedule of Butyrate glycerides on the growth performance and carcass composition of broiler chickens. *Poultry Science, 96*, 3221–3228.

Belviranlı, M., Gökbel, H., Okudan, N., & Başaral, K. (2012). Effects of grape seed extract supplementation on exercise-induced oxidative stress in rats. *British Journal of Nutrition, 108*(2), 249–256.

Cheah, K. Y., Howarth, G. S., & Bastian, S. E. (2014). GSE dose-responsively decreases disease severity in a rat model of mucositis; concomitantly enhancing chemotherapeutic effectiveness in colon cancer cells. *PLoS ONE, 9*, e85184.

Elbassiouni, F. E., Salim, E. I., & Zineldeen, D. H. (2018). The effect of the combination of cetuximab (Erbitux ®) and sodium butyrate on mucous secreting cells during rat colon carcinogenesis. *American Journal of Biology and Life Sciences, 6*(2), 18.

El-Kholy, A. A., Elkablawy, M. A., & El-Agamy, D. S. (2017). Lutein mitigates cyclophosphamide induced lung and liver injury via NF-κB/MAPK dependent mechanism. *Biomedicine & Pharmacotherapy, 92*, 519–527.

Salim *et al. The Journal of Basic and Applied Zoology*   (2023) 84:24

Page 10 of 10

Ghareeb, A., Moawed, F., Ghareeb, D., & Kandil, E. (2018). Potential prophylactic effect of berberine against rat colon carcinoma induced by 1,2-dimethyl hydrazine. *Asian Pacific Journal of Cancer Prevention, 19*(6), 1685–1690.

Guo, F., Hu, Y., Niu, Q., et al. (2018). Grape seed proanthocyanidin extract inhibits human esophageal squamous cancerous cell line ECA109 via the NF-κB signaling pathway. *Mediators of Inflammation*, *2018*, 3403972

Gupta, M., Dey, S., Marbaniang, D., Pal, P., Ray, S., & Mazumder, B. (2020). Grape seed extract: Having potential health benefits. *Journal of Food Science and Technology, 57*(4), 1205–1215.

Hsu, S. M., Raine, L., & Fanger, H. (1981). Use of avidin-biotin-peroxidase complex (ABC) in immunoperoxidase techniques: A comparison between ABC and unlabeled antibody (PAP) procedures. *Journal of Histochemistry and Cytochemistry, 29*, 577–580.

Jang, B., Yang, I.-H., Cho, N.-P., Jin, B., Lee, W. W., et al. (2019). Down-regulation and nuclear localization of survivin by sodium butyrate induce caspase-dependent apoptosis in human oral mucoepidermoid carcinoma. *Cancer Research, 88*, 160–167.

Jia, J., Nie, L., & Liu, Y. (2020). Butyrate alleviates inflammatory response and NF-κB activation in human degenerated intervertebral disc tissues. *International Immunopharmacology, 78*, 106004.

Kruh, J. (1981). Effects of sodium butyrate, a new pharmacological agent, on cells in culture. *Molecular and Cellular Biochemistry, 42*(2), 65–82.

Li, W., Wang, Q. L., Liu, X., Dong, S. H., Li, H. X., et al. (2015). The combined use of vitamin D3 and metformin exhibits synergistic chemopreventive effects on colorectal neoplasia in rats and mice. *Cancer Prevention Research (philadelphia, Pa.), 8*(2), 139–148.

Ma, N., Abaker, J. A., Bilal, M. S., Dai, H., & Shen, X. (2018). Sodium butyrate improves antioxidant stability in sub-acute ruminal acidosis in dairy goats. *BMC Veterinary Research, 14*(1), 275.

Manju, V., Balasubramaniyan, V., & Nalini, N. (2005). Rat colonic lipid peroxidation and antioxidant status: The effects of dietary luteolin on 1,2-dimethylhydrazine challenge. *Cellular & Molecular Biology Letters, 10*, 535–551.

Mao, J. T., Smoake, J., Park, H., Lu, Q., & Xue, B. (2016). GSE procyanidin extract mediates antineoplastic effects against lung cancer via modulations of prostacyclin and 15-HETE eicosanoid pathways. *Cancer Prevention Research, 12*, 925–932.

McNabney, S. M., & Henagan, T. M. (2017). Short chain fatty acids in the colon and peripheral tissues: A focus on butyrate, colon cancer, obesity and insulin resistance. *Nutrients, 9*(12), 1348.

Medina, V., Afonso, J. J., Alvarez-Arguelles, H., Hernández, C., & González, F. (1998). Sodium butyrate inhibits carcinoma development in a 1,2-dimethylhydrazine-induced rat colon cancer. *JPEN Journal of Parenteral and Enteral Nutrition, 22*(1), 14–17.

Rodríguez-Pérez, C., García-Villanova, B., Guerra-Hernández, E., & Verardo, V. (2019). Grape seeds proanthocyanidins: An overview of in vivo bioactivity in animal models. *Nutrients, 11*(10), 2435.

Roncucci, L., Pedroni, M., Vaccina, F., Benatti, P., Marzona, L., & De Pol, A. (2000). Aberrant crypt foci in colorectal carcinogenesis. Cell and crypt dynamics. *Cell Proliferation, 33*(1), 1–18.

Sadik, N. A. H., & Shaker, O. G. (2013). Inhibitory effect of a standardized pomegranate fruit extract on Wnt signaling in 1,2-dimethylhydrazine induced rat colon carcinogenesis. *Digestive Diseases and Sciences, 58*(9), 2507–2517.

Saleem, T. H., Eldein, H., & Mohamed, E. (2019). Effect of curcumin-containing chitosan nanoparticle on caspase-3, carcinoembryonic antigen in colorectal cancer induced by dimethylhydrazine. *Journal of Current Medical Research and Practice, 4*(3), 302–307.

Salim, E. I., El-Gamal, M. M., Mona, M. M., & Abdelhady, H. A. (2020). Attenuation of rat colon carcinogenesis by *Styela plicata* aqueous extract. modulation of NF-κB pathway and cytoplasmic Sod1 gene expression. *Asian Pacific Journal Cancer Prevention, 21*(9), 2739–2750.

Salim, E. I., Hegazi, M. M., Kang, J. S., & Helmy, H. M. (2016). Expression patterns of cancer stem cell markers during specific celecoxib therapy in multistep rat colon carcinogenesis bioassays. *Asian Pacific Journal of Cancer Prevention, 17*(3), 1023–1035.

Salim, E. I., Mahfouz, M. E., Kang, J. S., Hegazi, M. M., Helmy, H. M., & Eltonouby, E. A. (2019). Celecoxib targeted therapy attenuates mouse colon carcinogenesis through modulation of expression patterns of cancer stem cells. *Journal of Environmental Pathology, Toxicology and Oncology, 38*(4), 329–343.

Sharma, S. H., Kumar, J. S., Chellappan, D. R., & Nagarajan, S. (2018). Molecular chemoprevention by morin–A plant flavonoid that targets nuclear factor kappa B in experimental colon cancer. *Biomedicine & Pharmacotherapy, 100*, 367–373.

Sherif, A. A., Abdelhalim, S. Z., & Salim, E. I. (2017). Immunohistochemical and biochemical alterations following administration of proanthocyanidin extract in rats hepatocellular carcinoma. *Biomedicine & Pharmacotherapy, 93*, 1310–1319.

Shiraishi, N., Inai, Y., Bi, W., & Nishikimi, M. (2005). Fragmentation and dimerization of copper-loaded prion protein by copper-catalyzed oxidation. *The Biochemical Journal, 387*(Pt 1), 247–255.

Sohn, K. J., Puchyr, M., Salomon, R. N., et al. (1999). The effect of dietary folate on Apc and p53 mutations in the dimethylhydrazine rat model of colorectal cancer. *Carcinogenesis, 20*(12), 2345–2350.

Sung, H., Ferlay, J., Siegel, R. L., Laversanne, M., Soerjomataram, I., Jemal, A., & Bray, F. (2021). Global cancer statistics 2020: GLOBOCAN estimates of incidence and mortality worldwide for 36 cancers in 185 countries. *CA Cancer J Cin, 73*(3), 209–249.

Taylor, M. A., Khathayer, F., & Ray, S. K. (2019). Quercetin and sodium butyrate synergistically increase apoptosis in rat C6 and human T98G glioblastoma cells through inhibition of autophagy. *Neurochemical Research, 44*, 1715–1725.

Tu, X., Wang, M., Liu, Y., et al. (2019). Pretreatment of GSE extract exerts neuroprotective effect in murine model of neonatal hypoxic-ischemic brain injury by its antiapoptotic property. *Cellular and Molecular Neurobiology, 39*, 953–961.

Umesalma, S., & Sudhandiran, G. (2010). Differential inhibitory effects of the polyphenol ellagic acid on inflammatory mediators NF-κB, iNOS, COX-2, TNF-α, and IL-6 in 1,2-dimethylhydrazine-induced rat colon carcinogenesis. *Basic & Clinical Pharmacology & Toxicology, 107*, 650–655.

Vobornikova, I., & Pohanka, M. (2016). Smartphone-based colorimetric detection of glutathione. *Neuro Endocrinology Letters, 37*(Suppl1), 139–143.

Wendum, D., Masliah, J., Trugnan, G., & Fléjou, J. F. (2004). Cyclooxygenase-2 and its role in colorectal cancer development. *Virchows Archiv, 445*, 327–333.

Wu, R., Jiafu, F., Yuwei, Y., et al. (2017). Significance of serum total oxidant/antioxidant status in patients with colorectal cancer. *PLoS ONE, 12*(1), e0170003.

Yang, C., Wang, S., Liu, W., et al. (2020). Anthocyanidin extract from summerblack-grape affects the expression of Kl-67 in testis, ovary of D-Galactose-induced aging mice. *Journal of Oleo Science, 69*(4), 369–376.

Yoshioka, T., Kawada, K., Shimada, T., & Mori, M. (1979). Lipid peroxidation in maternal and cord blood and protective mechanism against activated oxygen toxicity in the blood. *American Journal of Obstetrics and Gynecology, 135*, 372–376.

Publisher's Note

Springer Nature remains neutral with regard to jurisdictional claims in published maps and institutional affiliations.